

Sensitivity analysis of the ECAE process via 2^k experiments design

Neil de Medeiros^I, Luciano Pessanha Moreira^I, José Divo Bressan^{II}, Jefferson Fabrício Cardoso Lins^I, Jayme Pereira de Gouvêa^I

^I Programa de Pós-graduação em Engenharia Metalúrgica, Universidade Federal Fluminense, Av. dos Trabalhadores, 420, CEP 27255-125, Volta Redonda RJ, Brazil

e-mail: neil@metal.eeimvr.uff.br ; luciano.moreira@metal.eeimvr.uff.br ; jfclins@metal.eeimvr.uff.br ; jpg@metal.eeimvr.uff.br

^{II} Centro de Ciências Tecnológicas (CCT/UEDESC), Campus Universitário, Bom Retiro CEP 89223-100, Joinville, SC, Brazil

e-mail: dem2jdb@joinville.udesc.br

ABSTRACT

In this work the theoretical solutions based upon the upper-bound theorem recently proposed by Pérez and Luri [Mech. Mater. 40 (2008) 617] for the equal channel angular extrusion process (ECAE) are analyzed by performing a 25 central composite factorial analysis. The uniaxial mechanical properties of commercial pure aluminium are considered by assuming isotropic nonlinear work-hardening combined to von Mises and Drucker isotropic yield criteria to predict the ECAE load and the effective plastic strain. From the proposed 25 factorial analysis, the main parameters affecting the ECAE pressure may be ranked as: (1) Friction factor, (2) die channels intersection angle, (3) outer and (4) inner die corners fillet radii and lastly, (5) plunger velocity. Alternatively, the effective plastic strain is mainly controlled by the die channels intersection angle and, in a less extent, by the outer and inner die corners fillet radii.

Keyword: Upper-bound theorem, factorial analysis, equal channel angular extrusion.

1 INTRODUCTION

The equal channel angular extrusion process (ECAE) is a severe plastic deformation process employed to produce bulk ultra-fine grained materials with improved mechanical properties [1, 2]. In the ECAE process, a well lubricated billet is forced to pass through a two-channel die with constant cross-sectional area. The workpiece undergoes a large amount of plastic strain by simple shear within the deformation zone located at the channels die intersection [3]. Thus, the knowledge of the kinematics of deformation is essential to understand the basic mechanisms controlling the grain refinement in the ECAE process. The consideration of material nonlinear work-hardening to predict the ECAE pressure, assuming a frictionless condition with an outer die corner radius, was firstly proposed by Alkorta and Sevillano [4]. Their analytical solution is based upon the upper-bound theorem and provides a good agreement with numerical predictions determined from a plane-strain finite element model. Later on, Pérez [5, 6] evaluated the effects of equal fillet die radii located at the die channels intersection with the help of the upper-bound theorem and finite element simulations, respectively. Although the analytical model proposed by Pérez neglected the effects of material work-hardening, the benefits of adopting a non-zero inner die corner radius were revealed up to a maximum value from which the predominant deformation mode is bending.

Eivani and Taheri [7] presented the first upper-bound solution in which both the friction conditions and nonlinear work-hardening behavior were considered for a die geometry containing only the outer die corner radius. By varying the die channels angle between 90° and 135° and for a given friction factor, they reported that both the effective von Mises plastic strain and normalized extrusion pressure decreases as the outer die corner radius increases. Besides, it is verified that the effect of the die channels intersection angle prevails over both tribological conditions and other geometrical or rheological parameters. Also, Eivani and Taheri [8] also analyzed the effects of the formation of a dead metal zone in sharp-corner dies and established an explicit dependence of the resulting strain per ECAE pass with the friction factor from the minimization of the extrusion force. A better agreement with the measured load was achieved by this recent work by comparison with the earlier results [7].

Pérez [5] and Luri *et al.* [9] developed theoretical expressions for the shear strain calculations considering all the possible die configurations. The authors showed a gain close to 11% of the effective plastic strain per pass when the inner radius is 2.67 times larger than the outer die fillet radius. Recently, Pérez and Luri [10] developed upper-bound solutions for the extrusion pressure, considering all die geometry possibilities and including the friction effects for perfectly plastic materials. The authors pointed out that the increasing of the inner fillet radius leads to an elevation of effective plastic strain combined with higher extrusion pressure levels.

Based upon the review presented here above, it is clear the need for more general modelling techniques to describe the effects of the relevant parameters on the strains and mechanical properties resulting from the ECAE, namely, tooling geometry, billet material, friction conditions and processing velocity. Into this context, the present work firstly aims at providing a sensitivity analysis with the help of the 2K central composite factorial design to evaluate the influence of these parameters on the effective plastic strain and the extrusion pressure for commercial pure aluminum and some typical die configurations by means of the variance analysis.

2 ECAE THEORETICAL MODELLING

2.1 Extrusion pressure

The upper-bound solutions developed by Pérez and Luri [10] for the extrusion pressure, p , for all possible die geometries and including frictional effects are recalled. The tooling configurations are shown in Figure 1 where the inner and outer fillet radii are defined by R_{inner} and R_{outer} , respectively, and have local origin along line O. At the same time, Φ is the die channels intersection angle whereas β denotes the angle associated to nonzero fillet radii values. Also, r and x define the radial and horizontal directions.

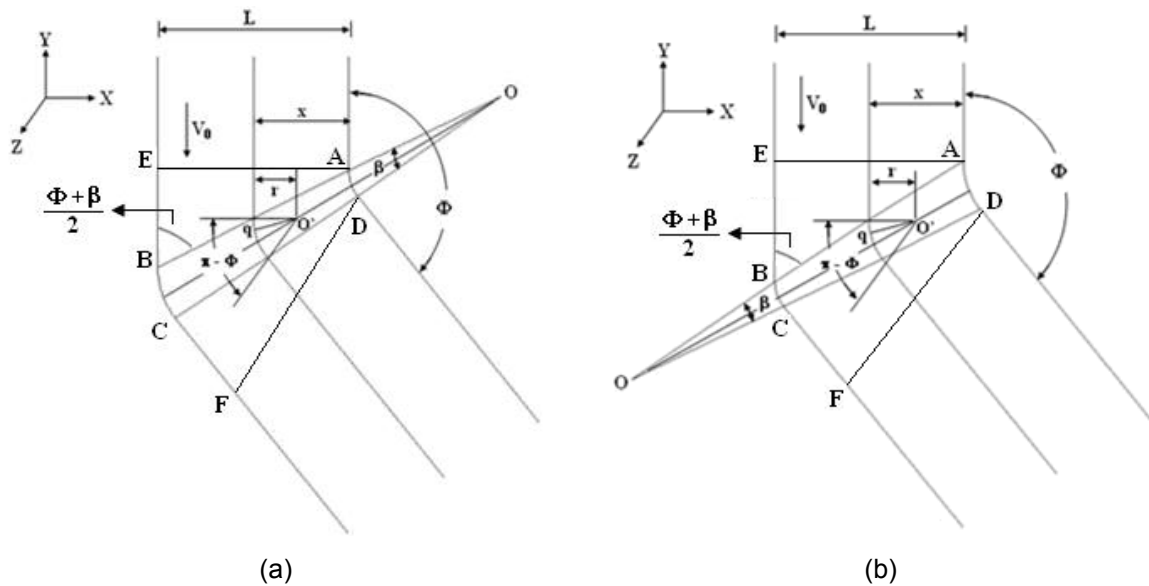


Figure 1: Die design for the extrusion pressure analytical solutions: (a) $R_{inner} < R_{outer}$ and (b) $R_{inner} > R_{outer}$.

Considering the material point q and its position vector \overline{Oq} and assuming the constant velocity V_0 hypothesis for both the plunger and the point q , the extrusion pressure of rectangular samples can be calculated by,

$$p = \kappa \left\{ \frac{(\pi - \Phi)}{\sin\left(\frac{\Phi + \beta}{2}\right)} + f \left[\frac{2H}{L} + (\pi - \Phi) \left(\frac{R_{inner} + R_{outer}}{L} \right) \left(1 - \frac{1}{\sin\left(\frac{\Phi + \beta}{2}\right)} + \frac{2H}{W} \right) \right] \right\} \quad R_{inner} < R_{outer} \quad (1a)$$

$$p = \kappa \left\{ \frac{(\pi - \Phi)}{\sin\left(\frac{\Phi - \beta}{2}\right)} + f \left[\frac{2H}{L} + (\pi - \Phi) \left(\frac{R_{inner} + R_{outer}}{L} \right) \left(1 - \frac{1}{\sin\left(\frac{\Phi - \beta}{2}\right)} \right) + \frac{2H}{W} \right] \right\} \quad R_{inner} > R_{outer} \quad (1b)$$

where κ is the material pure shear yield stress and f is the Tresca's friction factor. Also, H , L and W denote the billet total height, width and thickness, respectively.

According to Pérez and Luri [10] the angle β is given by,

$$\beta = 2 \arctan \left\{ \frac{(R_{outer} - R_{inner}) \tan(\Phi / 2)}{L + (R_{inner} - R_{outer}) + L \tan^2(\Phi / 2)} \right\} \quad \text{for } R_{inner} < R_{outer} \quad (2a)$$

$$\beta = 2 \arctan \left\{ \frac{(R_{inner} - R_{outer}) \tan(\Phi / 2)}{L + (R_{inner} - R_{outer}) + L \tan^2(\Phi / 2)} \right\} \quad \text{for } R_{inner} > R_{outer} \quad (2b)$$

2.2 Plastic Material Behaviour

The billet material plastic behaviour is assumed as isotropic and temperature independent including nonlinear work-hardening with strain-rate effects. Moreover, the yield surface shape influence on the pure shear yield stress κ and, therefore, on the extrusion pressure is evaluated by considering both von Mises and Drucker [11] isotropic yield criteria. Thus, the plastic loading condition is defined as,

$$f(\sigma_{ij}, \bar{\epsilon}^p, \dot{\bar{\epsilon}}^p) = F(\sigma_{ij}) - \sigma_y(\bar{\epsilon}^p, \dot{\bar{\epsilon}}^p) = 0 \quad (3)$$

where f denotes the yield function, $F(\sigma_{ij})$ is a first degree homogeneous function of the Cauchy stress tensor, $\sigma_{ij} = \sigma_{kk}\delta_{ij} + S_{ij}$, defining the yield surface shape whereas σ_y is the uniaxial yield stress identified as a function of the equivalent plastic strain and strain-rate scalar measures.

The von Mises and Drucker yield criteria are defined for the second and third invariants of the deviatoric stress components of the Cauchy stress tensor, S_{ij} , that is,

$$F(\sigma_{ij})_{\text{Mises}} = \sqrt{\frac{3}{2} S_{ij} S_{ij}} \quad (4a)$$

$$F(\sigma_{ij})_{\text{Drucker}} = (3 J_2)^{1/2} \left[1 - c \left(\frac{J_3^2}{J_2^3} \right) \right]^{1/6} = F(\sigma_{ij})_{\text{Mises}} \left[1 - c \left(\frac{J_3^2}{J_2^3} \right) \right]^{1/6} \quad (4b)$$

And assuming in-plane pure shear ($S_{12} = S_{21} = \kappa$ other $S_{ij} = 0$) combined with Equation 3,

$$\kappa_{\text{vonMises}} = \frac{\sigma_y}{\sqrt{3}} \quad (5a)$$

$$\kappa_{\text{Drucker}} = \left\{ \frac{1}{\sqrt{3}} \left[1 - \left(\frac{4c}{27} \right) \right]^{1/6} \right\} \sigma_y \quad (5b)$$

where c is a material constant satisfying the condition $-27/8 \leq c \leq 2.25$ [12] for the yield locus convexity. Drucker's yield criterion is suited to describe the crystallographic yield loci of both isotropic f.c.c. and b.c.c. metals. In the present work, the parameter c is assumed to be equal to 2.0. This value has been adopted by Ferron *et al.* [13] to fit the isotropic f.c.c. yield loci determined by Barlat and Lian [14] with the Bishop and Hill [15] model.

The uniaxial tension yield stress σ_y is calculated by means of the average stress obtained from the material Swift hardening law with multiplicative strain-rate sensitivity as,

$$\sigma_y = \bar{\sigma} = \frac{1}{\bar{\varepsilon}^{-p}} \int_0^{\bar{\varepsilon}^{-p}} \left[B(\varepsilon_0 + \varepsilon^p)^n \left(\frac{\varepsilon^p}{t_D} \right)^m \right] d\varepsilon^p \quad (6)$$

wherein $\bar{\varepsilon}^{-p}$ is the effective plastic strain, and the strain-rate effect is accounted for by introducing the dwelling time in the ECAE deformation zone, t_D , defined in section 2.3. Also, B , ε_0 , n and m denote strength coefficient, pre-strain, work-hardening exponent and strain-rate sensitivity exponent, respectively. Equation. 6 is numerically solved through the trapezoidal rule in order to accurately determine the mean stress. It should be noted that Equation 6 is restricted to a constant strain-rate deformation process. This assumption is adopted hereafter based upon the idea of a total time resulting from the ECAE deformation zone geometry. In the following, we assume that the elastic strains are small in comparison to the resulting plastic strains from the ECAE process and can, thus be neglected.

2.3 Effective plastic strain

The plastic strain-rate components are determined assuming isotropic work-hardening from the associated flow rule applied to the yield function, see Equation 3, as,

$$\dot{\varepsilon}_{ij}^p = \dot{\lambda} \frac{\partial f}{\partial \sigma_{ij}} = \dot{\lambda} \frac{\partial F}{\partial \sigma_{ij}} \quad (7)$$

where $\dot{\lambda}$ denotes the plastic multiplier. It is well known that both von Mises and Drucker plasticity criteria are first-degree homogeneous stress functions. Thus, by applying the Euler identity combined to the equivalent plastic work-rate on the Equation 7, one can verify that the plastic multiplier is equal to the effective plastic strain rate $\dot{\varepsilon}^{-p}$ conjugated of the effective stress measure $\bar{\sigma}$. In this way, the effective plastic strain defined in terms of the von Mises yield criterion is obtained by multiplying both sides of Equation 7 by $\dot{\varepsilon}_{ij}^p$ that is,

$$\dot{\varepsilon}^{-p} = \sqrt{\frac{2}{3} \dot{\varepsilon}_{ij}^p \dot{\varepsilon}_{ij}^p} \quad (8)$$

where the Equation 8 is valid to von Mises and Drucker criteria, once for a pure shear stress state the third invariant of the tensor S_{ij} vanishes. Therefore, the total effective plastic strain is obtained by integrating Equation 8, namely,

$$\bar{\varepsilon}^{-p} = \int_{t_0=0}^{t_D} \sqrt{\frac{2}{3} \dot{\varepsilon}_{ij}^p \dot{\varepsilon}_{ij}^p} dt \quad (9)$$

And, considering that for in-plane pure-shear stress state $2 \dot{\varepsilon}_{ij}^p = \dot{\gamma}^p$ and assuming a constant shear strain-rate as $\dot{\gamma}^p = (\dot{\gamma}^p / t_D)$ one obtains:

$$\bar{\varepsilon}^p = \frac{1}{\sqrt{3}} \gamma^p \quad (10)$$

where, according to Figure 1, the plastic shear strain-rate components are defined as V_0 / x by assuming $x = L$ into the regions AEB and DFC. Also, for the portion ABCD the associated shear strain contribution is equal to V_0 / r [10]. The solutions for the shear plastic strain associated to die geometries presented in Figure 1 were proposed by Pérez [5] and Luri *et al.* [9], that is,

$$\gamma^p = 2 \cotan\left(\frac{\Phi + \beta}{2}\right) + (\pi - \Phi) \left[1 - \cotan\left(\frac{\Phi + \beta}{2}\right) \tan\left(\frac{\Phi}{2}\right) \right] \quad \text{for } R_{\text{inner}} < R_{\text{outer}} \quad (11a)$$

$$\gamma^p = 2 \cotan\left(\frac{\Phi - \beta}{2}\right) + (\pi - \Phi) \left[1 - \cotan\left(\frac{\Phi - \beta}{2}\right) \tan\left(\frac{\Phi}{2}\right) \right] \quad \text{for } R_{\text{inner}} > R_{\text{outer}} \quad (11b)$$

2.4 Deformation time

In the present work, the during which the billet undergoes severe plastic deformation along the die channels intersection was assumed as the contributions from the regions AEB, ABCD and DFC depicted on Figure 1 by considering that the inlet and outlet surfaces AE and DF have the same length. Thus, for the continuous kinematically admissible velocity field defined by a constant velocity V_0 , the time between the inlet and outlet surfaces is given by,

$$t_D = \frac{L}{V_0} \left\{ 2 \cotan\left(\frac{\Phi + \beta}{2}\right) + \frac{(\pi - \Phi)}{L} \left[1 - \cotan\left(\frac{\Phi + \beta}{2}\right) \tan\left(\frac{\Phi}{2}\right) \right] \left[R_{\text{inner}} + L \left(1 - \cotan\left(\frac{\Phi + \beta}{2}\right) \tan\left(\frac{\Phi}{2}\right) \right) \right] \right\} \quad R_{\text{inner}} < R_{\text{outer}} \quad (12a)$$

$$t_D = \frac{L}{V_0} \left\{ 2 \cotan\left(\frac{\Phi - \beta}{2}\right) + \frac{(\pi - \Phi)}{L} \left[1 - \cotan\left(\frac{\Phi - \beta}{2}\right) \tan\left(\frac{\Phi}{2}\right) \right] \left[R_{\text{inner}} + L \left(1 - \cotan\left(\frac{\Phi - \beta}{2}\right) \tan\left(\frac{\Phi}{2}\right) \right) \right] \right\} \quad R_{\text{inner}} > R_{\text{outer}} \quad (12b)$$

2.5 The 2^K Factorial Central Composite Factorial Design

The methodology proposed by Montgomery [16] for the single-replicate 2^K central composite design of experiments is adopted for theoretical simulations to classify the interesting parameters influence on both extrusion pressure and effective plastic strain by means of a variance analysis. The parameters considered are die geometry (Rinner, Router and Φ), friction conditions (Tresca friction factor f) and plunger velocity (V_0). These parameters and their corresponding values are listed in Table 1.

Table 1: Parameters for the ECAE 2K factorial design.

Parameter	Letter for the combinations	Adopted levels				
		Low	Center	Axial ⁻	Axial ⁺	High
R_{outer} (mm)	(a)	3.5	5.5	0.7432	10.2568	7.5
R_{inner} (mm)	(b)	3.5	5.5	0.7432	10.2568	7.5
Φ (degrees)	(c)	90	105	69.5	140.35	120
f	(d)	0.08	0.12	0.02486	0.21514	0.16
V_0 (mm / s)	(e)	2.5	3.75	0.7776	6.723	5.0

Also, the rotatability parameter α is considered when the central and axial points are added on the factorial analysis. Thus, for the 25 central composite design we have,

$$\alpha = \pm \sqrt[4]{2^5} \cong \pm 2.3784 \quad (13)$$

To perform the variance analysis related to central composite factorial design, the calculations of parameters effect (A, B, ..., K), sum of the squares (SS_{A,B, ..., K}) for each individual effect, total sum of squares (SS_{T_{A,B, ..., K}}), pure quadratic curvature SSPQ, error (E) and mean error are needed. The Equations 14 to 19 define each one of these variables, that is,

$$A, B, \dots, K = \frac{2 \text{sum}(a, \dots, abcdef)}{nr 2^K} \quad (14)$$

$$SS_{A, B, \dots, K} = \frac{(S_{A, B, \dots, K})^2}{nr 2^K} \quad (15)$$

$$SS_{T_{A, B, \dots, K}} = \sum_{i=1}^2 \sum_{j=1}^2 \sum_{K=1}^2 y_{ijk}^2 - \frac{y_{ijk}^2}{nr 2^K} \quad (16)$$

$$SS_{PQ} = \frac{n_F n_{CP} (\bar{y}_F - \bar{y}_{CP})}{n_F + n_{CP}} \quad (17)$$

$$E = SS_{T_{A, B, \dots, K}} - \sum_{l=I}^N SS_l - SS_{PQ} \quad (18)$$

$$\bar{E} = \frac{E}{DOF_{I, \dots, N}} \quad (19)$$

where nr, n_F, n_{CP}, \bar{y}_F and \bar{y}_{CP} denote number of replicates, numbers of factorial and central points, averages between factorial and central points, respectively.

Finally, the variance, F_o, is defined by,

$$F_o = \frac{SS_l}{\bar{E}} \quad (20)$$

where the index l takes into account from I to N-th value in the summation over the most important effects on either p or ε denoted by SS_l. Also, the combinations between the considered parameters for each case simulated are listed on Table 2.

Table 2: Combinations for the 25 factorial design treatment*.

Treatments	Coded factors *				
	R _{outer}	R _{inner}	Φ	f	V ₀
1	-1	-1	-1	-1	-1
a	1	-1	-1	-1	-1
b	-1	1	-1	-1	-1
c	-1	-1	1	-1	-1
d	-1	-1	-1	1	-1
e	-1	-1	-1	-1	1
ab	1	1	-1	-1	-1
ac	1	-1	1	-1	-1
ad	1	-1	-1	1	-1
ae	1	-1	-1	-1	1
bc	-1	1	1	-1	-1
bd	-1	1	-1	1	-1
be	-1	1	-1	-1	1
cd	-1	-1	1	1	-1
ce	-1	-1	1	-1	1
de	-1	-1	-1	1	1
abc	1	1	1	-1	-1
abd	1	1	-1	1	-1
abe	1	1	-1	-1	1
acd	1	-1	1	1	-1
ace	1	-1	1	-1	1
ade	1	-1	-1	1	1
bcd	-1	1	1	1	-1
bce	-1	1	1	-1	1
bde	-1	1	-1	1	1
cde	-1	-1	1	1	1
abcd	1	1	1	1	-1
abce	1	1	1	-1	1
abde	1	1	-1	1	1
acde	1	-1	1	1	1
bcde	-1	1	1	1	1
abcde	1	1	1	1	1
Central point	0	0	0	0	0
Axial ⁻ : R _{outer}	-2.3784	0	0	0	0
Axial ⁺ : R _{outer}	2.3784	0	0	0	0
Axial ⁻ : R _{inner}	0	-2.3784	0	0	0
Axial ⁺ : R _{inner}	0	2.3784	0	0	0
Axial ⁻ : Φ	0	0	-2.3784	0	0
Axial ⁺ : Φ	0	0	2.3784	0	0
Axial ⁻ : f	0	0	0	-2.3784	0
Axial ⁺ : f	0	0	0	2.3784	0
Axial ⁻ : V ₀	0	0	0	0	-2.3784
Axial ⁺ : V ₀	0	0	0	0	2.3784

* - 1= "low" ; 0 = "center"; -2.3784 = "axial⁻"; 2.3784 = "axial⁺"; 1 = "high"

3 RESULTS AND DISCUSSION

The mechanical properties considered in the present work are related to the commercial pure aluminium tested in uniaxial tension by Bressan *et al.* [17], according to Equation. (6), defined by B = 235 MPa, ε₀ = 0.045, n = 0.21 and m = 0.027. Firstly, an evaluation of the adopted yield criteria and friction effects on the extrusion pressure, p, is realized assuming a die with Φ = 90° wherein the die fillet radii are taken equal to zero together with a plunger velocity (V₀) value of 2.5 mm / s. Then, a 2K central composite factorial design is employed to classify, in order of relevance, the die geometrical, frictional conditions and process parameters upon the predictions of either p and assuming the billet dimensions as H = 75 mm and L = W = 15 mm. The levels assumed for each parameter are listed in the Tab. 1.

Table 3: Combinations for the 25 factorial design treatment.

Source of variance	Sum of squares		Degrees of Freedom		Mean square		Fo	
	p (MPa)	$\bar{\epsilon}^p$	p (MPa)	$\bar{\epsilon}^p$	p (MPa)	$\bar{\epsilon}^p$	p (MPa)	$\bar{\epsilon}^p$
Main effects								
A (Router)	3354.613484	0.013763313	1	1	3354.61348	0.013763313	0.63052866	0.53328489
B (Rinner)	2540.422764	0.020234735	1	1	2540.42276	0.020234735	0.477494463	0.784032039
C (□)	147977.2759	1.818131421	1	1	147977.276	1.818131421	27.81361072	70.4468481
D (f)	193720.0477	0.000621995	1	1	193720.048	0.000621995	36.41136089	0.024100351
E (V0)	463.1281321	0.000621995	1	1	463.128132	0.000621995	0.087048944	0.024100351
2 factors	-	-	-	-	-	-	-	-
AB	10.96155461	0.000623089	1	1	10.9615546	0.000623089	0.002060319	0.024142735
AC	1333.252108	0.009000828	1	1	1333.25211	0.009000828	0.250596282	0.348753646
AD	0.286393932	0.000622807	1	1	0.28639393	0.000622807	5.38302E-05	0.024131794
AE	0.293721652	0.000622807	1	1	0.29372165	0.000622807	5.52075E-05	0.024131794
BC	1010.606521	0.009003914	1	1	1010.60652	0.009003914	0.189952249	0.348873226
BD	3.882144835	0.000621995	1	1	3.88214484	0.000621995	0.000729683	0.024100351
BE	0.222432828	0.000621995	1	1	0.22243283	0.000621995	4.18082E-05	0.024100351
CD	315.5369051	0.000622807	1	1	315.536905	0.000622807	0.059307894	0.024131794
CE	12.95651113	0.000622807	1	1	12.9565111	0.000622807	0.002435288	0.024131794
DE	16.9616313	0.000621995	1	1	16.9616313	0.000621995	0.003188086	0.024100351
3 factors	-	-	-	-	-	-	-	-
ABC	3.70769399	0.000621713	1	1	3.70769399	0.000621713	0.000696893	0.02408942
ABD	0.063314433	0.000622807	1	1	0.06331443	0.000622807	1.19005E-05	0.024131794
ABE	0.000959768	0.000622807	1	1	0.00095977	0.000622807	1.80397E-07	0.024131794
ACD	0.386801023	0.000621995	1	1	0.38680102	0.000621995	7.27026E-05	0.024100351
ACE	0.116736046	0.000621995	1	1	0.11673605	0.000621995	2.19416E-05	0.024100351
ADE	2.50774E-05	0.000622807	1	1	2.5077E-05	0.000622807	4.71351E-09	0.024131794
BCD	0.907500191	0.000622807	1	1	0.90750019	0.000622807	0.000170573	0.024131794
BCE	0.088486042	0.000622807	1	1	0.08848604	0.000622807	1.66317E-05	0.024131794
BDE	0.000339927	0.000621995	1	1	0.00033993	0.000621995	6.38922E-08	0.024100351
CDE	0.027627542	0.000622807	1	1	0.02762754	0.000622807	5.19284E-06	0.024131794
4 factors	-	-	-	-	-	-	-	-
ABCD	0.003135805	0.000621995	1	1	0.00313581	0.000621995	5.89402E-07	0.024100351
ABCE	0.000324628	0.000621995	1	1	0.00032463	0.000621995	6.10166E-08	0.024100351
ABDE	5.54445E-06	0.000622807	1	1	5.54445E-06	0.000622807	1.04213E-09	0.024131794
ACDE	3.38665E-05	0.000621995	1	1	3.3866E-05	0.000621995	6.36549E-09	0.024100351
BCDE	7.94682E-05	0.000622807	1	1	7.9468E-05	0.000622807	1.49367E-08	0.024131794
5 factors	-	-	-	-	-	-	-	-
ABCDE	2.74541E-07	0.0006	1	1	2.7454E-07	0.000621995	5.16023E-11	0.024100351
Pure quadratic	66.034	0.0006	-	-	66.034	-	-	-
Absolute error	1.7025E+05	0.8259	32	32	5320.3188	0.0258	-	-
TOTAL	180581.5835	2.7128	31	31	-	-	-	-

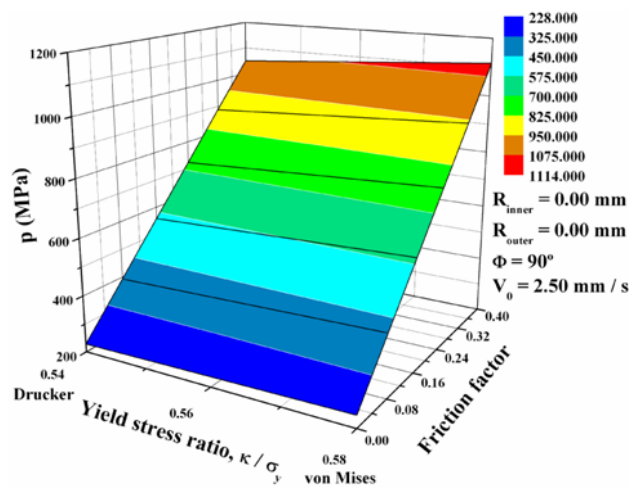


Figure 2: Influence of yield criterion and friction conditions on the pressure.

Figure 2 presents the effects of the plasticity criterion defined in terms of the ratio κ/σ_y equal to 0.54 for Drucker and 0.58 for von Mises isotropic descriptions and the friction factor f on the ECAE pressure assuming $\Phi = 90^\circ$, $R_{inner} = R_{outer} = 0$ mm along with $V_0 = 2.5$ mm / s. As expected, one can observe the existence of a direct effect from the frictional conditions, namely, the ECAE pressure increases significantly with the friction factor f or in a less extent with the yield stress ratio κ/σ_y . The Drucker yield surface presents a flattening between plane tension/compression and pure shear stress states which is responsible for the decreasing of the ratio κ/σ_y in comparison to the von Mises yield criterion. Hereafter, the Drucker isotropic yield criterion is adopted for all the analysis related to factorial analysis on the pressure predictions.

Table 3 presents the variance (F_0) analysis associated to the 25 central composite design employed in the present work. In relation to the pressure, p , the influence of the parameters considered for the factorial design can be classified in order of importance as: (1) friction factor m , (2) intersection die angle Φ , (3) outer fillet radius R_{outer} , (4) inner fillet radius R_{inner} and (5) the plunger velocity V_0 , respectively. As expected, in the case of the effective plastic strain the variance results confirmed the large dependence only with the die geometrical parameters ordered as: (1) intersection die angle Φ , (2) inner fillet radius R_{inner} and (3) outer fillet radius R_{outer} .

4 CONCLUSIONS

Analytical investigations based upon the upper-bound method, including the material strain-rate effects and two isotropic plasticity yield criteria are proposed in the present work in order to evaluate the extrusion pressure and the effective plastic strain associated to the processing of a commercial pure aluminium. The effects of the plasticity criteria on the extrusion pressure are evaluated to point out the formulation responsible to processing load decreasing. Finally, a variance analysis based on the 2⁵ central composite factorial design was performed to quantify the relevance of these parameters on the ECAE pressure and the effective plastic strain. From these analyses, the following conclusions can be outlined:

1) The analysis of the influence of yield surface shape and friction conditions on the extrusion pressure proved to be a useful tool to better understand the frictional conditions effects arising from a single pass of ECAE at room temperature. In particular, the isotropic Drucker yield criterion is more appropriate to reproduce the pure shear and plane tension /compression stress states than the von Mises criterion and, thus, should be adopted in the analytical predictions of fcc materials deformed via ECAE;

2) From the performed variance analysis, the ECAE parameters most affecting the extrusion pressure can be classified in the following order of importance: (1) friction factor, (2) intersection die channels angle, (3) outer fillet radius, (4) inner fillet radius and (5) the plunger velocity, respectively. Also, for the effective plastic strain the significance order for the affecting parameters is: (1) intersection die channels angle, (2) inner fillet radius and (3) outer fillet radius.

5 ACKNOWLEDGEMENTS

Neil de Medeiros and Luciano P. Moreira thank to CAPES for the research grant of the Post-Doctoral Program (PNPD). Luciano P. Moreira also acknowledges FAPERJ (Jovem Cientista do Nosso Estado, 2008).

6 REFERENCES

- [1] SEGAL, V.M. "Materials processing by simple shear", *Materials Science and Engineering A*, v. 197, pp. 157-164, 1995.
- [2] IWAHASHI, Y., WANG, W., NEMOTO, M., LANGDON, T.G. "Principle of equal-channel angular pressing for the processing of ultra-fine grained materials", *Scripta Materialia*, v. 35, pp. 143-146, 1996.
- [3] SEGAL, V.M. "Severe plastic deformation: simple shear versus pure shear", *Materials Science and Engineering A*, v. 338, pp. 331-344, 2002.
- [4] ALKORTA, J., SEVILLANO, J.G.A. "Comparison of FEM and upper-bound type analysis of equal-channel angular pressing (ECAP)", *Journal of Materials Processing Technology*, v. 141, pp. 313-318, 2003.

- [5] PÉREZ, C.J.L. “On the correct selection of the channel die in ECAP processes”, *Scripta Materialia*, v. 50, pp. 387-393, 2004.
- [6] PÉREZ, C.J.L. “Upper bound analysis and FEM simulation of equal fillet radii angular pressing”, *Modelling and Simulation in Materials Science and Engineering*, v. 12, pp. 205-214, 2004.
- [7] EIVANI, A.R., KARIMI TAHERI, A. “An upper bound solution of ECAE process with outer curved corner”, *Journal of Materials Processing Technology*, v. 182, pp. 555-563, 2007.
- [8] EIVANI, A.R., KARIMI TAHERI, A. “The effect of dead metal zone formation on strain and extrusion force during equal channel angular extrusion”, *Computational Materials Science*, v. 42, pp. 14-20 2008.
- [9] LURI, R., PÉREZ C.J.L., LEÓN J. A. “New configuration for equal channel angular extrusion dies”, *Journal of Manufacturing Science and Engineering*, v. 128, pp. 860-865, 2006.
- [10] PÉREZ, C.J.L., LURI R. “Study of the ECAE process by the upper bound method considering the correct die design”, *Mechanics of Materials*, v. 40, pp. 617-628, 2008.
- [11] DRUCKER, D.C. “Relation of experiments to mathematical theories of plasticity”, *Journal of Applied Mechanics*, v. 16, pp. 349-357, 1949.
- [12] CAZACU, O., BARLAT, F. “Generalization of Drucker's Yield Criterion to Orthotropy”, *Mathematics and Mechanics of Solids*, v. 6, pp. 613-630, 2001.
- [13] FERRON, G., MAKKOUK, R., MORREALE, J. “A parametric description of orthotropic plasticity in metal sheets”, *International Journal of Plasticity*, v. 10, pp. 431-449, 1994.
- [14] BARLAT, F., LIAN, J. “Plastic behavior of sheet metals. Part I: A yield function for orthotropic sheets under plane stress conditions”, *International Journal of Plasticity*, v. 5, pp. 51-66, 1989.
- [15] BISHOP, J.F.W., HILL, R. “A theory of the plastic distortion of a polycrystalline aggregate under combined stresses”, *Philosophical Magazine*, v.42, pp. 414-427, 1951.
- [16] MONTGOMERY, D.C. “Design and Analysis of Experiments”, *John Wiley & Sons*, New York, 1997.
- [17] BRESSAN, J.D., UNFER, R.K. “Construction and validation tests of a torsion test machine”, *Journal of Materials Processing Technology*, v. 179, pp. 23-29, 2006.